Journal of
Ship&Ocean
Technology
©DECEMBER 2004

SOTECH Vol. 8, No. 4, pp. 34~44, 2004

Feasibility Study on Quartz Liner Application for Marine Diesel Engine Visualization

Kyo Seung Lee[1], Moon Yeal Baek[2] and Dennis N. Assanis[2]

[1] Kyonggi Institute of Technology, Gyeonggi-Do, Korea; E-mail; leeks@kinst.ac.kr
[2] The University of Michigan, Michigan, U.S.A.

Abstract

Engine visualization is the most important process to develop the new engine. But this step has a major difficulty that is almost impossible to access the engine on running. Therefore, little indication from the experimental and analytical results has been so far. This work has conducted the important issue of developing a quartz liner. And it has given us good qualitative and quantitative results of temperature and stress fields in the quartz cylinder by considering forced convection of outside quartz liner, thickness of the quartz liner and pre-heating effect to operate quartz engine safely.

Keywords: quartz liner, visualization, FEM, stress, convection heat transfer

1 Introduction

Engine visualization is the most important process to develop the new engine by Namazian et al(1980). But this step has a major difficulty that is almost impossible to access the engine on running. To visualize inside engine cylinder without any interference, the material of engine cylinder has to be transparent, strong, resistant to thermal stress and able to withstand high temperature. Quartz has been considered seriously as a cylinder material in order to visualize in-cylinder gas motion because of their special material properties.

Quartz is the optical material most commonly used both for commercial purpose and research. The cylinder made of quartz is frequently broken during the engine operation because quartz is very fragile when handled. Quartz is totally different material from conventional engine material, for instance cast-iron or aluminum composite materials.

The effort to visualize engine cylinder began with a glass cylinder by Otto in 1872. Withrow and Rassweiler(1936) and later Nakanishi et al(1975) were used quartz window mounted L-head engines and photographed combustion phenomena. Holtman and McClure(1978) visualized diesel engine flows by a single cylinder with a thick(2.2mm), fused quartz cylinder and operated this engine under motored and limited number of fired cycle condition. A single cylinder research engine made of a 1.72mm thick quartz liner for flow visualization was built by Bates(1988) and used for motoring studies. He reported that one of quartz liner survived for 11 months of intermittent operation while accumulating some large chips on the top from mounting errors and some small chips on the bottom from assembly errors. And it finally failed due to thermal stress after a 25 minute motoring test.

In previous works reviewed, the optical engine design was a compromise between optical access and engine components. Therefore it is needed to clarify the thermal and

mechanical behavior of quartz liner and to identify the best configuration.

In this study, to find the optimum quartz liner configuration, the steady and transient temperature fields of quartz liner were conducted. And then the steady and the transient stress fields were examined with effects of forced cooling, thickness and pre-heating under the motoring and firing conditions.

2 FEM analysis

2.1 Modeling and basic assumptions

A 3-dimensional finite element model of the quartz liner was composed and a total of 8,320 nodes and 700 elements were employed to describe the FE model using cartesian coordinate. The baseline liner was modeled as a cylinder (height = 124.8, thickness = 13.625, outer dia. = 119.25, inner dia. = 92). On the inside surface of the cylinder, heat loss from the combustion gas and heat generation by ring friction were applied. On the outside surface, cooling either by natural or by foreced convection was applied. All grids are isoparametric 8-node solid brick. Steady state and transient heat transfer, and stress analyses were accomplished using the commercial codes Hypermesh 3.0(pre- and post-processor) and ABAQUS 5.8(solver). In this work, temperature dependent material properties were used and material properties are summarized in Table 1. The heat transfer analysis was conducted first. Subsequently, the heat transfer results and combustion pressure were used to perform the stress analysis.

Table 1: Material properties of the quartz liner

Density, ρ , [kg/m^3]	2.2 x 10^3
Young's Modulus, E, [GPa]	70
Poisson's Ratio, v	0.17
Specific Heat, c_p, [J/kg·K]	100 °C 772 500 °C 964 900 °C 1052
Thermal Conductivity, k, [W/m·K]	20 °C 1.36 100 °C 1.46 200 °C 1.55 300 °C 1.67 400 °C 1.84 950 °C 2.88
Thermal Expansion Coefficient, β , [1/K x 10^{-7}]	100 °C 5.1 200 °C 5.8 300 °C 5.9 600 °C 5.4 900 °C 4.8

During the real engine operation, engines are under time varying coupled thermal load (due to heat input from combustion and friction) and mechanical load (due to clamping forces and combustion pressure). To describe realistic engine operating condition by FEM analysis, several reasonable assumptions are needed. In this study, engine operation was assumed to be quasi-steady state at given time step and cyclic thermal shock effect in

thermal penetration depth was ignored. Combustion pressure and heat fluxes were assumed to be constant profiles in time, but varied along the liner longitudinal direction from the liner top. Frictional heat source was assumed to be stepwise function. Figure 1 shows schematic diagram of imposed boundary conditions.

2.2 Boundary conditions

The cylinder was modeled with specified top and bottom temperatures. And in order to impose thermal and mechanical boundary conditions, FEM model was divided by several regions (see Figure 1) and details are shown in Table 2. A1-A6 and F1-F22 indicate areas where boundary conditions were imposed and %s indicate applied heat fluxes from combustion(Qw) and friction(Qf).

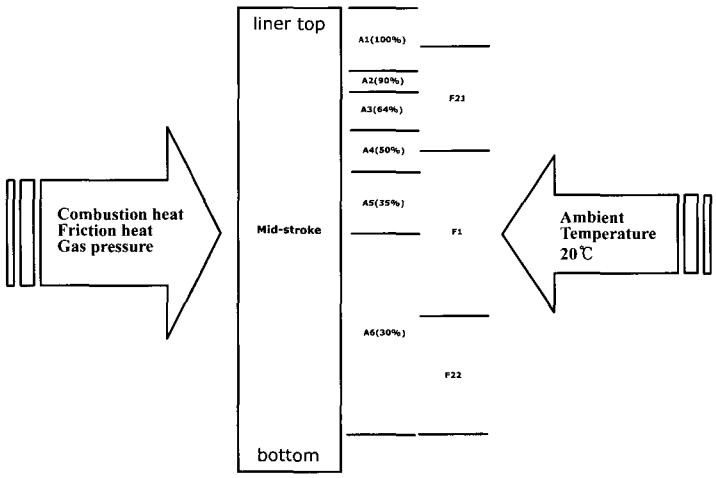

Figure 1: Schematic diagram of the quartz liner for boundary conditions

Thermal and mechanical boundary conditions and constraints

(a) Heat flux from combustion gas to the liner, Qw

In this case, it was assumed to be 10% of $m_f Q_{LHV}$ because there is no heat loss to cylinder head for firing condition suggested by GM Motors(2000) and based on experiment.

$$\dot{m}_f = 1.13 \text{ kg/h}$$

$$Q_{w,fire} = 511522.6 \text{ W/m}^2$$

For motoring, the total heat transfer loss from the gas is equal to the integral of P*dV* during a cycle. The amount of heat going into the liner was assumed to be 1/3 of the total value suggested by GM Motors(2000) and based on experiment.

$$Q_{w,motor} = 7444.4 \text{ W/m}^2$$

(b) Heat flux to liner due to friction, Q_f

Heat transfer come from friction is basically 1.5% of $\dot{m}_f Q_{LHV}$ for firing condition suggested by GM Motors(2000) and based on experiment.

$$Q_{f,fire} = 6925 \text{ W/m}^2$$

And also it was assumed to be about 70% based on experimental data for motoring condition of the firing condition value.

$$Q_{f,motor} = 4640 \text{ W/m}^2$$

(c) Heat transfer coefficient for natural convection, h

Vertical flat plate correlation was used for the fired and motored operation by Incropera et al(1985).

Table 2: Thermal and mechanical boundary conditions

		Motoring / Applied	Firing / Applied
Heat flux from gas to wall Qw, [W/m2]	A1	7444.4 / 3722.2	51152.3 / 25576.2
	A2	6700.0 / 3350.0	46037.1 / 23018.6
	A3	4764.0 / 2382.0	32737.5 / 16368.8
	A4	3722.2 / 1861.1	25576.2 / 12788.1
	A5	2605.5 / 1861.1	17903.3 / 8951.7
	A6	2233.3 / 1116.7	15345.7 / 7672.9
Friction heat input Qf, [W/m2]	F1	/ 4617.3	/ 6925.0
	F21,22	/ 2308.7	/ 3463.0
Convection heat transfer coefficient h, [W/mK]	Natural C.	7.7	9.9
	Forced C. I	23.8	31.5
	Forced C. II	38.5	52.2
		Motoring	Firing
In-cylinder gas pressure P, [kPa]	A1	2000	6000
	A2	1800	5000
	A3	1500	3500
	A4	1000	2000
	A5	500	800

(d) Heat transfer coefficient for forced convection I (moderate cooling), h

Equation around the cylinder shaped object was used for both of the fired and motored operation by Incropera et al(1985). It was assumed that $V_{nozzle} = 1$ *m/s* for moderate cooling and 5 m/s for intensive cooling. And also nozzle diameter was assumed to be 0.1 *m*.

(f) Coolant temperature

The coolant temperature in head and bottom were assumed to 90°C and 30°C, respectively.

(g) In-cylinder gas pressure in kPa

During the motoring, it was assumed as if hydrostatic pressure distribution along the longitudinal direction of the liner based on experimental data. While, there are no firing data, it was also assumed, based on similar engine operating conditions.

(h) Mechanical constraints

As mechanical constraints for the stress analysis, some nodes located in top and bottom were fixed ($\Delta x = \Delta y = \Delta z = 0$).

(i) Engine operating condition

Engine speed is 1200 rpm and full load condition.

3 Validation of FEM model

In order to validate the FEM model, transient temperature at the selected points of thermal field were compared with measurements recorded at the same points.

3.1 Engine set-up

A single quartz cylinder was used for this experiment and the specification of engine shown in Table 3. Three thermocouples were located at outside quartz cylinder. The hi means 5 mm away, mid means 55 mm away, and low means 82 mm away from the lir top, respectively. The temperature was recorded under the following conditions; motored 1200 rpm, 30°C intake air temperature and 90°C cylinder head coolant temperatu 100kPa manifold pressure, and uncharacterized air jet as external forced cooling.

Table 3: Specification of test engine

Bore	Stroke	Con. rod	Liner length	thickness	Comp. ratio
92mm	96mm	223.5mm	124.8mm	13.625mm	9.5

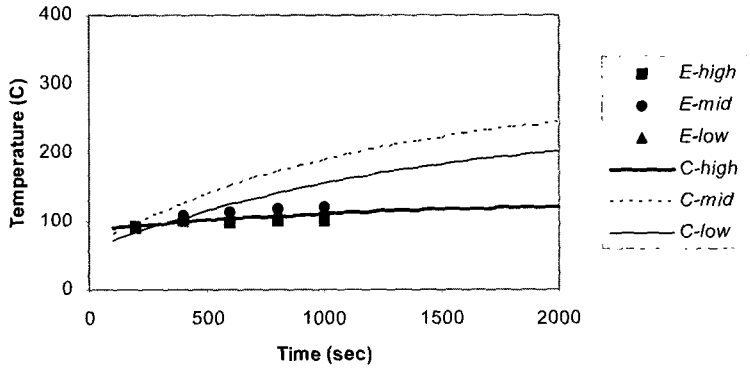

Figure 2: Comparison between measured and predicted transient outside surface temperature of quartz liner under natural convection condition. (E : Experiment C : Computation)

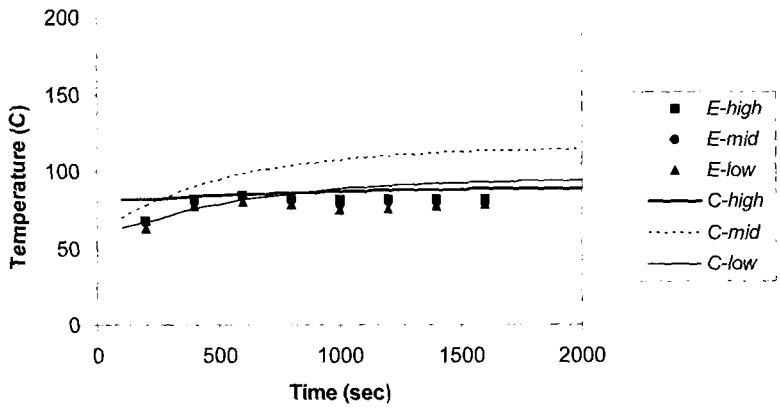

Figure 3: Comparison between measured and predicted transient outside surface temperature of quartz liner under cooled condition. (E : Experiment C : Computation)

3.2 Temperature field comparison

Measured and predicted surface temperatures at given locations, 5(high), 55(mid), and 82(low) mm away from the liner top, were compared in Figures 2 and 3, and E- and C- indicate experiment and computational data, respectively. In general, predicted data are larger than those of experiment. Under the natural convection condition, the highest temperature achieved from experiment is recorded at the mid-point, followed by low and high as well as computation data. But some differences in magnitude are observed. Under the cooled condition, the highest temperature achieved from experiment is recorded at the high-point, followed by low and mid. On the other hand, the order of magnitude of computation data is mid, low and high-points. Though there are some differences in order of magnitude, each value is satisfactory. The discrepancies above can be attributed to the following reasons. First, there is some possibility of maldistribution of cooling air-jet under cooled condition. Generally, under the motoring condition, main heat source is friction. Hence, the temperature of mid-stroke is expected higher than that of other location. Second, there are lots of assumptions to impose thermal boundary conditions because of lack of basic experimental data about combustion phenomena in quartz engine and so on. However, the FEM model of this study has the potential to capture the thermal and stress fields within the quartz liner with acceptable accuracy.

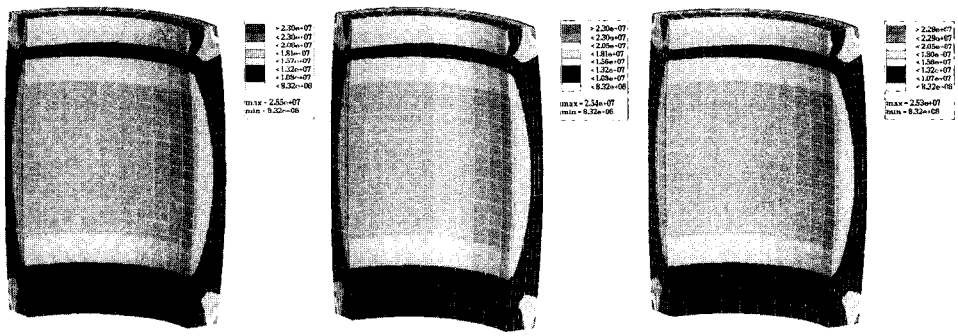

(a) (b) (c)

Figure 4: Transient thermal stress[MPa] distribution of the quartz liner with deformation at 10 second after staring of firing
(a) natural convection (no cooling)
(b) forced convection I (moderate cooling)
(c) forced convection II (intensive cooling)

4 Stress distribution

4.1 Effect of forced cooling

The effects of natural convection, moderate forced convection and intensive forced convection were examined in order to validate effectiveness of forced cooling. FEM predictions of transient thermal stress distribution in the quartz liner are shown in Figures 4 to 7 for several time step and the results are summarized in Table 4. The (a), (b) and (c) indicate the case of no cooling, moderate forced cooling and intensive forced cooling, respectively. Through Figures 4 to 7, while the general characteristic of iso-stress distribution was almost same, the magnitude of stress and deformation increased gradually as time is increasing. Higher stress concentration region was observed on the outside

surface of the top and bottom and maximum thermal stress was observed in that region. And inside surface of the quartz liner has also slightly higher level of thermal stress.

Table 4: Summary of forced cooling effect - maximum thermal stress [MPa]

	1 sec	10 sec	100 sec	912 sec	2180 sec	Steady State
Natural Convection	25.3	25.5	29.5	54.4	64.8	67.1
Forced Convection I	25.3	25.4	28.8	46.6	50.6	51.0
Forced Convection II	25.3	25.3	28.2	41.7	43.7	43.8

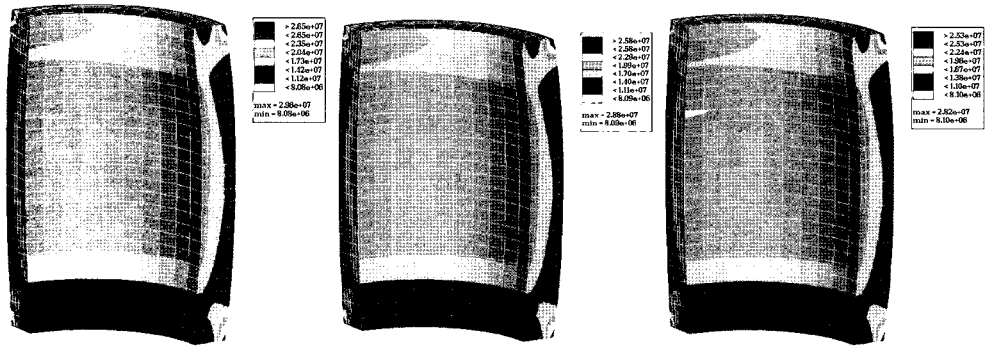

(a) (b) (c)

Figure 5: Transient thermal stress[MPa] distribution of the quartz liner with deformation at 100 second after staring of firing
(a) natural convection (no cooling)
(b) forced convection I (moderate cooling)
(c) forced convection II (intensive cooling)

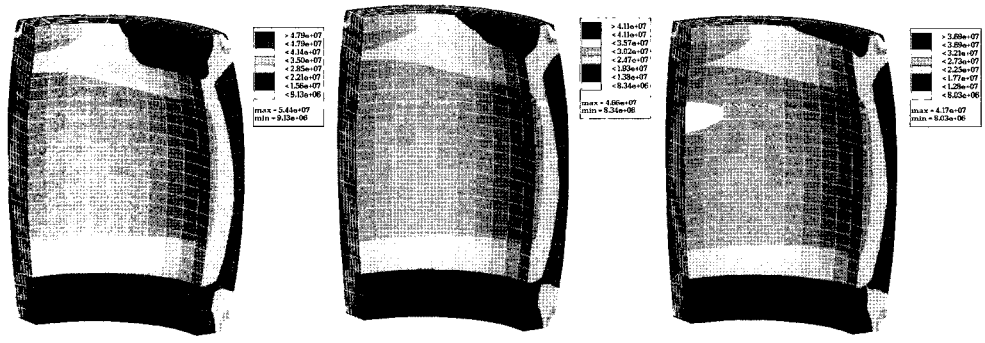

(a) (b) (c)

Figure 6: Transient thermal stress[MPa] distribution of the quartz liner with deformation at 912 second after staring of firing
(a) natural convection (no cooling)
(b) forced convection I (moderate cooling)
(c) forced convection II (intensive cooling)

At the early stage of combustion (before 100 second), the magnitude and the maximum thermal stress level was almost same on each cases. But as time passed, the difference between each case increased gradually and then at steady-state, the maximum thermal stress of no cooling case is 153% of that of intensive cooling and the moderate cooling case is 117%. Therefore, forced cooling of the outside quartz liner is very helpful to decrease the maximum thermal stress level.

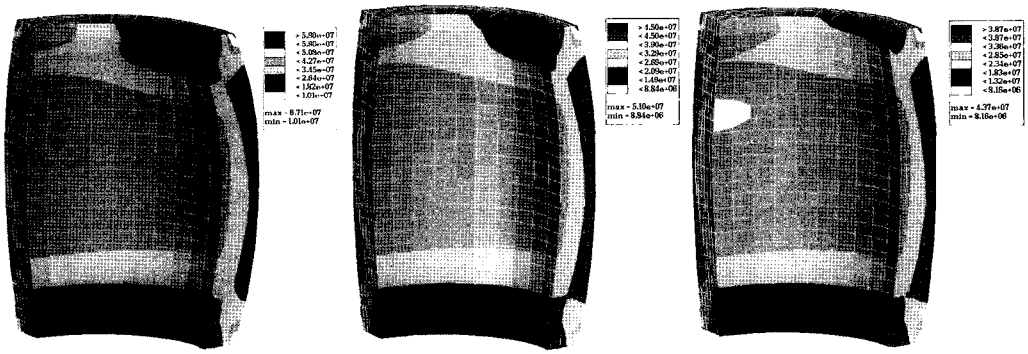

(a) (b) (c)

Figure 7: Steady-state thermal stress[MPa] distribution of the quartz liner with deformation
(a) natural convection (no cooling)
(b) forced convection I (moderate cooling)
(c) forced convection II (intensive cooling)

4.2 Effect of liner thickness

The liner thickness was changed from the baseline engine to investigate the effect on stress distribution. As shown in Table 5, for stress due to thermal, the thinner the thickness of the quartz liner was, the smaller the stress level became, because temperature distribution became more uniform. Hence thermal stress decreased gradually.
For stress due to combustion pressure, the thicker the thickness of the quartz liner was, the smaller the stress level became. Because of the effect of reinforcement, i.e., a safety factor was increased.

Table 5: Summary of thickness effect, steady-state stress [MPa]

Model thickness	Stress due to thermal	Stress due to combustion pressure	Combined stress
10 mm	42.4	23.0	58.6
11.5 mm	43.0	20.2	56.6
13.625 mm	43.8	17.4	54.6
15.5 mm	44.3	15.5	53.4
17.0 mm	44.5	14.4	52.5

For stress due to both thermal and combustion pressure, the thicker the thickness of the quartz liner was, the smaller the stress level became gradually, because the rate of decreasing for stress due to thermal was smaller than that of mechanical stress caused from combustion pressure.

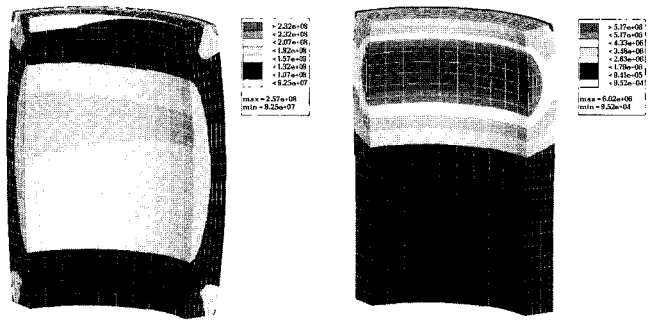

(a) (b)

Figure 8: Steady-state stress [MPa] distribution of the stainless steel liner, motoring
(a) thermal loading (b) mechanical loading

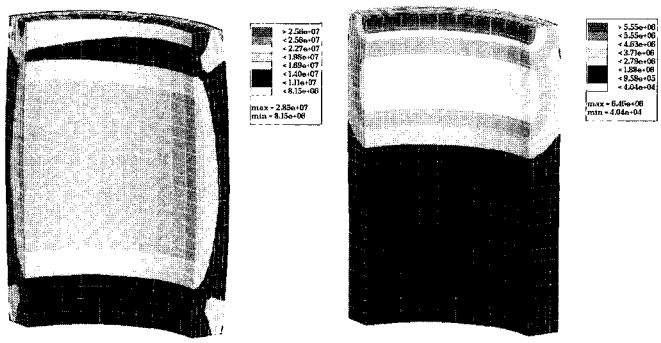

(a) (b)

Figure 9: Steady-state stress [MPa] distribution of the quartz liner, motoring
(a) thermal loading (b) mechanical loading

4.3 Effect of thermal loading and mechanical loading

In order to investigate the relative importance between thermal and mechanical loading, the results of the stainless steel liner and the quartz liner were compared in Figures 8 to 11. Figures 8 and 9 are shown the predicted stress distribution of stainless steel liner and the quartz liner during motoring operation, respectively. While some difference was observed in magnitude, general trend of distribution and deformation was very similar.

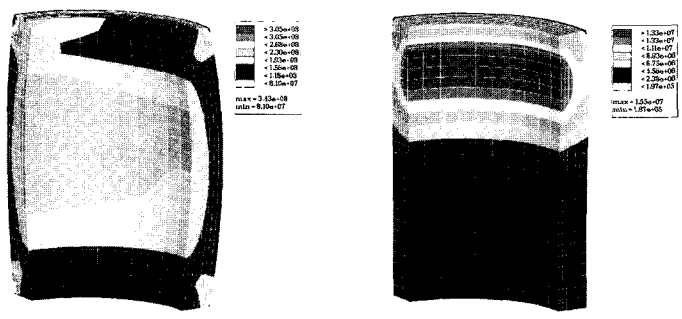

(a) (b)

Figure 10: Steady-state stress [MPa] distribution of the stainless steel liner, firing
(a) thermal loading (b) mechanical loading

For both stainless steel and quartz cases, the effect of mechanical loading was negligible. Figures 10 and 11 are shown the predicted stress distribution of stainless steel liner and the quartz liner during firing operation, respectively.

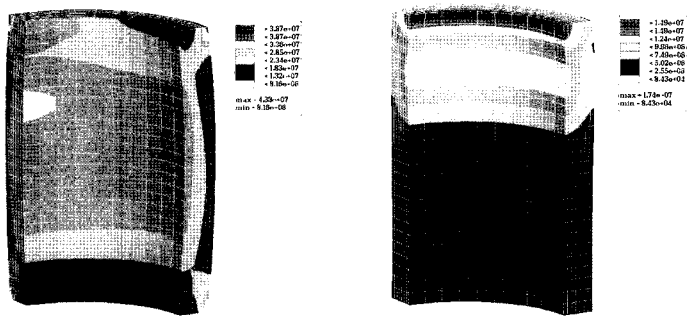

(a) (b)

Figure 11: Steady-state stress [MPa] distribution of the quartz liner, firing
(a) thermal loading (b) mechanical loading

General trend of distribution and deformation was still similar to those of motoring case except the propagation of higher stress level region. For the stainless steel liner, the effect of mechanical loading was still negligible. For the quartz liner, however, stress due to combustion pressure is not negligible any more and the relative magnitude of mechanical stress due to combustion pressure was 37.9% of that of thermal stress. Hence, for the quartz liner, mechanical stress should be considered deliberately.

4.4 Effect of pre-heating

The effects of pre-heating were investigated for different 4 cases to decrease the maximum stress, primarily thermal stresses as show in Table 6. There was no pre-heating effect.

Table 6: Summary of pre-heating effect [MPa]

model	1 sec	2 sec	3.5 sec	5.75 sec	9.12 sec	10 sec
No Pre-heat	32.8	32.8	32.9	32.9	33.0	33.0
Heat Lamp	36.0	36.0	36.0	36.0	36.0	36.1
Motoring	39.3	39.3	39.3	39.2	39.2	39.2
Light Firing	44.5	44.4	44.3	44.1	44.0	44.0

5 Conclusions

There has been little indication from the experimental and analytical results, which is capable of causing a sudden quartz cylinder breaking. This work has conducted the important issue of developing a quartz liner. And it has given us good qualitative and quantitative results of temperature and stress fields in the quartz cylinder. The following conclusions drawn from this study can be useful for improving current quartz engine technique:

- Forced convection of outside quartz liner is very helpful to decrease the thermal stress level.

- To find the optimal thickness of the quartz liner is basic design problem. So it should be determined with considering of strength, price and other reasons.
- For conventional engine materials, mechanical loading due to combustion pressure is negligible. However, for the quartz liner, the relative magnitude of mechanical stress takes a large portion of total stress. Hence, the mechanical stress should be considered deliberately.
- There is no pre-heating effect. Eventually, more intensive forced cooling would rather be desirable than pre-heating in order to decrease stress level.

Acknowledgment

The author gratefully acknowledges partial financial support by the Ministry of Education and Human Resources Development (2004 Junior College Financial Support Program).

Reference

Bates, S.C. 1988. A transparent engines for flow and combustion visualization studies. SAE 880520, 1-13.

GM Motors, Deer Born Lab., Private Communication 2000.

Incropera, F.P. and J.W. Dewitt. 1985. Introduction to Heat Transfer, 2nd Edition. John Wiley & Sons.

Nakanishi, K., T. Hirano, T. Inoue and S. Ohigashi. 1975. The effect of charge dilition on combustion and its improvement flame photograph Study, 1-23.

Namazian, M., S. Hansen, E. Lyford-Pike, J. Sanchez-Barsse, John B. Heywood and J. Rife. 1980. Schlieren visualization of the flow and density fields in the cylinder of a spark-ignition engines. SAE 800044, 1-18.

Withrow, L. and G.M. Rassweiler. 1936. Slow-motion shows knocking and non-knocking explosion. SAE Transaction, **39**, 297-303.